Journal of Alloys and Compounds 525 (2012) 34–38

Contents lists available at SciVerse ScienceDirect

Journal of Alloys and Compounds

journal homepage: www.elsevier.com/locate/jallcom

Ferri- to ferro-magnetic transition in the martensitic phase of a Heusler alloy

L.H. Bennett[a], V. Provenzano[b,*], R.D. Shull[b], I. Levin[b], E. Della Torre[a], Y. Jin[a]

[a] Institute for Magnetics Research, George Washington University, Washington D.C. 20052, USA
[b] Material Measurements Laboratory, National Institute of Standards and Technology, Gaithersburg, MD 20899, USA

ARTICLE INFO

Article history:
Received 29 December 2011
Received in revised form 4 February 2012
Accepted 6 February 2012
Available online xxx

Keywords:
Heusler alloys
First-order magneto-structural transformation
Ferri-to-ferromagnetic transition
Conventional and inverse magnetocaloric effects
Magnetic hysteresis

ABSTRACT

During the past decade the magnetic properties of Heusler alloys have been extensively studied, motivated in part by the observation of large magnetocaloric effects (MCEs) displayed by these alloys near room temperature. We present new data and develop a consistent mechanism to explain the complex hysteretic behavior of a $Ni_{50}Mn_{35}In_{15}$ Heusler alloy. The magnetization of this alloy is characterized by two critical temperatures. Below the lower critical temperature, the alloy is a *ferrimagnetic* martensite. Between the two critical temperatures, the alloy is a *ferromagnetic* martensite. Above the higher critical temperature, it is a *paramagnetic* austenite. The transitions at both critical temperatures are first order. The ferri-to-ferromagnetic transition and the crystallographic martensite-to-austenite transition explain the various facets observed in the M_{ZFC} and M_{FC} vs. T plots and their variations with increasing magnetic field. The model successfully explains the isothermal M vs. H loops near room temperature, whose behavior is strongly dependent on the initial magnetic state.

1. Introduction

The magnetic properties of Heusler shape memory alloys have been the subject of many studies. These studies have been motivated in part by the observation of large magnetocaloric effect (MCE) peaks displayed by these [1–6] and related [7–9] alloys near-room temperature. The structure and magnetic properties of the stoichiometric $Ni_{50}Mn_{25}Ga_{25}$ alloy have been of particular interest to a number of research groups. They concluded that this alloy, on heating, undergoes a first-order magnetocrystalline transition from tetragonal martensite to a cubic austenite structure at a transformation temperature, T_M, ranging from 175 K to 220 K; followed by a second-order ferromagnetic–paramagnetic transition identified with a Curie temperature of the austenite phase, T_C, between 375 K and 380 K; the transitions are reversible with temperature [10,11]. Later it was found [12–16] that the supposed transition temperatures, T_M and T_C, could made nearly coincident either by doping the alloy with Co or Cu or by slightly varying the alloy composition in the off-stoichiometric form of $Ni_{50+X}Mn_{25-X-Y}Ga_{25+Y}$, with $X \approx 5$ and $Y \approx$ l–2. The isothermal magnetization versus field loops displayed large hysteresis losses and the magnetization characteristics indicative of a field-induced magneto-structural phase transformation [17–22].

More recently, the structure and the magnetic properties of the off-stoichiometric Heusler alloy and related alloys have generated much interest because their unusual and complex magnetic properties [23–28], including the presence of a larger inverse magnetocaloric effect (MCE) peak [29] and a smaller conventional peak both occurring near room temperature as well as the display of large magnetoresistance at moderate field values [30]. Similar to what had been previously proposed for the Co or Cu-doped $Ni_{50}Mn_{25}Ga_{25}$ and the off-stoichiometric $Ni_{50}Mn_{25}Ga_{25}$ alloys, the presence of the inverse and conventional MCE peaks observed in the $Ni_{50}Mn_{35}In_{15}$ alloy is believed to be the result of the near-coincidence of two transformation temperatures both close to room temperature. That is, on heating, the Ni50$Mn_{35}In_{15}$ alloy has been assumed to undergo a first-order magneto-structural martensitic transformation from tetragonal martensite to ferromagnetic cubic austenite at T_M, followed by the ferromagnetic-to-paramagnetic second-order magnetic transition of the austenite phase at its Curie temperature, T_C [29–33].

The data presented by [34] is more appropriately interpreted (on heating) as a first order ferri-to-ferro-magnetic phase transition within the martensitic phase, followed by a magneto-structural transition from a martensitic to an austenitic phase at which the material becomes paramagnetic. The more recent studies by Bhobe et al. [35,36] on the phase structure and magnetic properties of the $Ni_{50}Mn_{35}In_{15}$ alloy by X-ray absorption fine structure (EXAFS) and SQUID magnetometry measurements seems to confirm that this alloy displays a cubic austenite B2 structure above 305 K and a tetragonal *L21* martensite structure below 302 K. The $Ni_{50}Mn_{35}In_{15}$

* Corresponding author. Tel.: +1 301 975 6042; fax: +1 301 975 4553.
E-mail address: virgil.provenzano@nist.gov (V. Provenzano).

0925-8388/$ – see front matter © 2012 Elsevier B.V. All rights reserved.
doi:10.1016/j.jallcom.2012.02.062

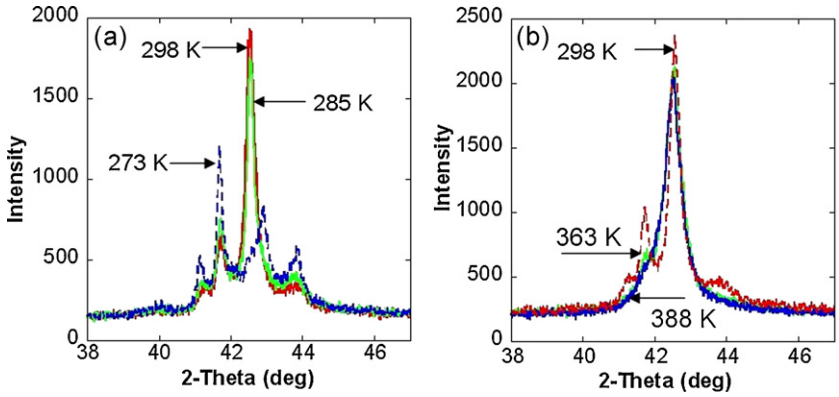

Fig. 1. X-ray diffraction patterns for the $Ni_{50}Mn_{35}In_{15}$ alloy recorded (a) on heating from 273 K to 298 K and (b) from 298 K to 388 K.

alloy undergoes a crystallographic phase transition, the details of which are affected by minute differences in the alloy composition, sample preparation, and heat treatment; however, the assumed near coincidence of T_M and T_C temperatures does not adequately account for the details of the complex magnetic behavior observed in this alloy as a function of both temperature and field. In this paper we present new magnetic data and provide a new a mechanism that accounts for the various features of this complex behavior.

2. Experimental methods

The $Ni_{50}Mn_{35}In_{15}$ alloy samples used for this study were prepared by arc melting appropriate amounts of the component elements using a water-cooled copper hearth in an argon atmosphere under ambient pressure. The sample was then homogenized for 2 h at 800 °C in an evacuated quartz tube and then quenched in ice water.

The microstructure, chemical composition, and phase structure of the alloy were then examined by energy dispersive spectroscopy (EDS), and X-ray diffraction, respectively. The EDS chemical analysis showed that the alloy composition was within 1% atom fraction of the target value of $Ni_{50}Mn_{35}In_{15}$. The magnetization data as a function of temperature at constant field values and as a function of field at constant temperatures were measured using a SQUID magnetometer.

3. Results and discussion

Fig. 1 is a summary of the X-diffraction data obtained on the $Ni_{50}Mn_{35}In_{15}$ alloy between 273 K and 388 K. The room temperature (298 K) data reveal a primary austenite phase with some amount of the martensite phase (Fig. 1a and b). The martensite phase persists in the sample on heating at least up to 363 K (Fig. 1b), whereas cooling the sample below room temperature results in the near disappearance of the austenite phase around 273 K (Fig. 1a). Therefore, the X-ray data presented in Fig. 1 clearly indicate the coexistence of the austenite and martensite phases in the temperature range from 273 K to 363 K. The details and significance of these mixed phase assemblages will be discussed elsewhere.

Fig. 2a shows the temperature dependence of the magnetization between 2 K and 390 K, measured on heating (M_{ZFC}), after the sample had been cooled in zero field from room temperature down to 2 K, and on cooling (M_{FC}) under an applied field of 4 kA/m (50 Oe) (Fig. 2a). The M_{ZFC} exhibits a rapid increase in the magnetization from ≈270 K to ≈285 K followed by a subsequent rapid decrease from ≈310 K to ≈320 K. The same M_{ZFC} plot shows also the presence of a peak at a lower temperature ($T_G \approx 190$ K), recognized as a spin glass peak. The corresponding M_{FC} vs. T plot at 4 kA/m and the M_{ZFC} and M_{FC} vs. T plots at higher field (Fig. 2b) that are presented and discussed in the following paragraphs provide additional evidence that the peak at ≈190 K is a spin glass peak.

The following observations can be made regarding the spin glass peak: (1) the center of the peak (T_G) shifts from 190 K to 160 K as the field is increased from 4 kA/m to 40 kA/m; and, as mentioned above, (2) the peak disappears for fields larger than 80 kA/m and is not present in the M_{FC} plots; (3) the magnetization values of the corresponding M_{FC} plot are somewhat higher than those of the M_{ZFC} plot from about 250 K down to T_G, below which the M_{ZFC} and M_{FC} plots begin to diverge, with M_{FC} monotonically increasing and M_{ZFC} monotonically decreasing; and (4) the decrease of T_G with increasing field, H, follows an H^{62} fit. This is close to the de Almeida–Thouless 2/3 power law that applies to spin glasses.

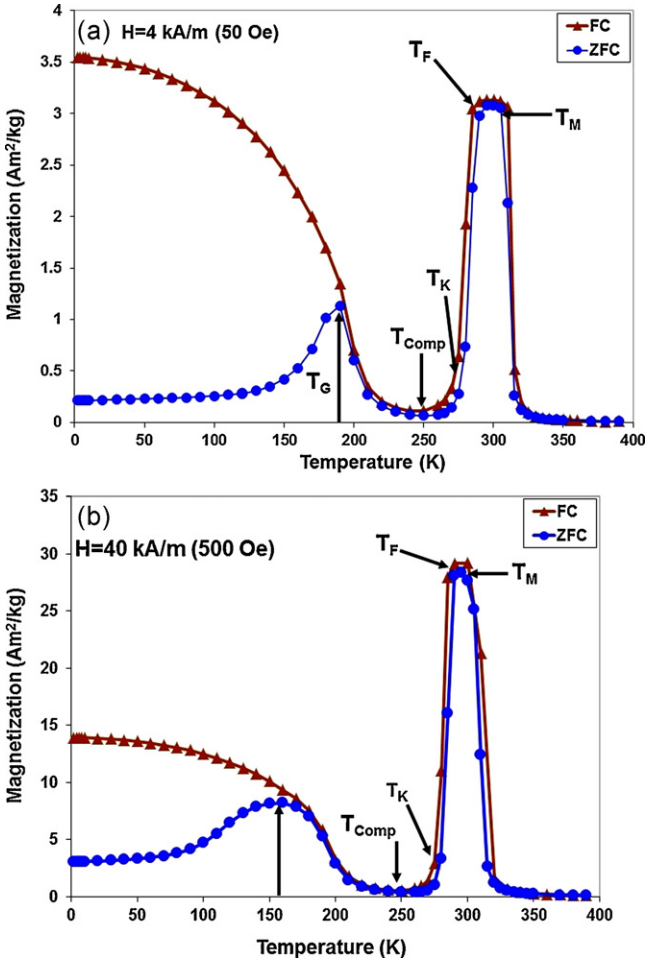

Fig. 2. M_{ZFC} and M_{FC} vs. T plots for the $Ni_{50}Mn_{35}In_{15}$ alloy measured under an applied field of (a) 4 kA/m (50 Oe) and of (b) 40 kA/m (500 Oe). The experimental uncertainty of the magnetic data is indicated by the size of the symbols in the M vs. T plots. The same uncertainty applies to magnetic data presented in Figs. 3 and 4.

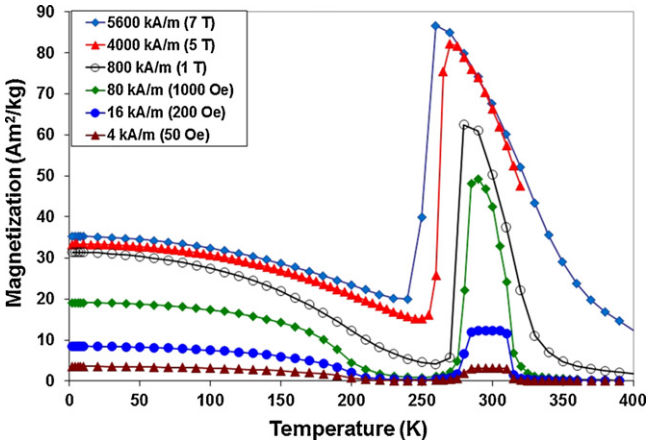

Fig. 3. M_{FC} vs. T plots for the $Ni_{50}Mn_{35}In_{15}$ alloy measured at different field values.

The M_{FC} vs. T plot at 4 kA/m shows that, as the temperature decreases from 390 K to 2 K, the plot retraces the M_{ZFC} plot from 390 K down to about 200 K. However, in this temperature range the M_{FC} values are slightly higher than the corresponding M_{ZFC} values, especially in the narrow temperature range between 320 K and 310 K where the magnetization exhibits a rapid increase; and between 285 K and 270 K, where the magnetization exhibits a rapid decrease. Therefore, in these two temperature ranges, the M vs. T plots each exhibits thermal hysteresis. As it will be discussed later, these two discontinuous changes in the magnetization are associated with two first-order transitions. At about 250 K, both M_{FC} and M_{ZFC} plots exhibit a minimum close to zero magnetization. From 250 K to 5 K the magnetization monotonically increases with decreasing temperature and, consequently, the lower temperature peak present in the M_{ZFC} plot is not present in the M_{FC} plot.

Fig. 2b shows that characteristics of the M_{ZFC} and M_{FC} plots at 40 kA/m (Fig. 2b) are similar to those at 4 kA/m (Fig. 2a), except, (1) the center of the lower temperature peak (T_G) in the M_{ZFC} plot has shifted to about 160 K and (2) the larger peak around 295 K shows a smaller flat region than the peak at 4 kA/m. But similar to the M_{ZFC} plot at the lower field, there is a rapid increase in the magnetization from 280 K to 295 K, followed by a rapid decrease from 295 K to 315 K. Finally, as evidenced by the higher values of M_{FC} compared to those of M_{ZFC}, between 315 K and 275 K, the magnetization displays a thermal hysteresis similar to that observed in the M vs. T plots at lower field value (Fig. 2a).

With regards to the higher temperature peak, the M_{FC} values are significantly higher compared to the corresponding M_{ZFC} values in the range of temperature between 310 K and 270 K. In this temperature range, the M vs. T plots show two sequential discontinuous changes in the magnetization, both on heating and cooling and the difference in the magnetization between M_{FC} and corresponding M_{ZFC} values give rise to thermal hysteresis in the these two narrow temperature regions where, on heating, the magnetization displays a rapid increase that is followed by rapid decrease; these two discontinuous changes in the magnetization (transitions) are reversed on cooling.

From M_{ZFC} and M_{FC} vs. T plots presented in Fig. 2, there is an indication that the center of the higher temperature peak shifts to lower temperatures with increasing fields. At first glance, the M_{FC} plots presented in Fig. 3 appear to provide additional evidence of this shift. In fact, the plots in Fig. 3 appear to suggest that the center of the higher temperature peak has shifted from 295 K at 4 kA/m down to about 260 K at 5600 kA/m (7 T) and further that with increasing field, the base of the peak broadens and it sharpens to a single point for field values of 80 kA/m or higher. However, though the higher temperature peak is well defined for field values of 40 kA/m and lower (refer to Fig. 2 plots), for field values of 80 kA/m and higher, what appears to be a well-defined peak, is not a peak at all but is simply the intersection of two first-order transitions that shift in tandem to lower temperatures with increasing field. This apparent peak represents the temperatures at which the magnetization attains its maximum value.

From the M vs. T plots the following can be stated more definitely. The M_{FC} plots presented in Fig. 3 clearly show that for field values of 80 kA/m or smaller the magnetization displays a minimum value around 250 K. Above 80 kA/m, the depth of the minimum decreases as the field value increases. This and other characteristics displayed by the M vs. T plots shown in Figs. 2 and 3 cannot be explained solely on the basis of the previously proposed and generally accepted mechanism involving a first- and a second-order sequential transitions at temperatures T_M and at T_C, respectively. Specifically, the previously proposed mechanism cannot clearly explain the following observations: (1) the magnetization minimum around 250 K; (2) the monotonically increasing magnetization in the M_{FC} plots below the without ever reaching a saturation value, even for high field values; and, (3) the shifting of the apparent higher temperature peak to lower temperatures for field values of 80 kA/m and higher. In this paper we propose a new mechanism to explain the magnetic data we obtained in the $Ni_{50}Mn_{35}In_{15}$ Heusler alloy. Unlike what has been previously proposed by a number of research groups, both in the US and abroad, who investigated the crystallography and magnetic behavior of the same and related Heusler alloys, we propose that the martensite phase at lower temperatures is a ferrimagnet (i.e., two sub-lattices of unequal magnetic moments aligned oppositely to one another), while at higher temperatures this phase converts to a ferromagnet in which the moments in the two sub-lattices are aligned parallel with each other. The fact that the martensite phase may present a ferrimagnetic ordering below a certain temperature is consistent with the study of Aksoy et al. who, from their magnetic and neutron data obtained on two Heusler alloys, have concluded seeing an antiferromagnetic alignment in the martensite phase [37].

Kittel [38] proposed a mechanism that emphasizes the first-order nature of the ferri- (or antiferromagnetic) transformation to ferromagnetic ordering within the same crystal structure which we define as the Kittel temperature, T_K. This phenomenon has been previously observed in other metallic systems [39,18,40,41]. The magnetization exhibits a minimum at≈250 K (Fig. 2a and b), which is identified as the compensation temperature (T_{Comp}) of the ferrimagnet. That is, at about 250 K, the spin moments of the two sub-lattices are equal and opposite. The Néel temperature of this ferrimagnet is not observed because it is above the Kittel temperature [38]. The M_{ZFC} plots in Fig. 2 show that above T_K the magnetization increases rapidly, reaching a maximum at $\approx T_F$. The maximum magnetization value at 40 kA/m is about two times larger than the highest magnetization value (reached at lowest temperature, 5 K) in the corresponding M_{FC} plot. This is consistent with a ferri-to-ferromagnetic transition taking place within the martensite phase. With further increases in temperature, the martensite phase undergoes a subsequent first order magneto-structural transition to the paramagnetic austenite phase between T_K and T_M. It follows, therefore, that these two sequential first-order transformations both involve the martensite phase. As the temperature is increased above T_M, the magnetization exhibits the paramagnetic characteristic of the austenitic phase. However, as noted earlier, the mixed phase assemblages are present between 273 K and 363 K; involving the nucleation and growth of the austenitic phase from the martensite phase. Above 363 K, the martensitic phase transforms completely to the austenitic phase (Fig. 1). In Fig. 2a and b, T_K, indicates the beginning of the ferri-to-ferromagnetic transformation that is manifested by a sudden

increase in the magnetization value that coincides with a sudden increase in the lattice dimensions within the martensite crystal structure [34].

The key features of the complex magnetic behavior displayed by the Ni50Mn35In15 alloy are all consistent with, and logically follow from our basic assumption that the martensite phase is a ferrimagnet at low temperatures and transforms into a ferromagnet near room temperature. Within the temperature range of 270 K to 285 K the ferri-to-ferromagnetic transformation of the martensite phase can be field-induced. This transformation within the martensite phase is a key difference from what has been previously proposed and our basic assumption that the steep rise in the magnetization observed in the M_{ZFC} vs. T plots, observed in Fig. 2, is due to a first-order transition occurring within the martensite phase. It follows, therefore, that the ferromagnetic behavior of the austenite phase is not manifested within the range of temperature studied. Our basic premise of the two sequential first-order transitions both involving the martensite phase is consistent with the thermal hysteresis present in the M vs. T plots presented in Fig. 2. The thermal hysteresis provides further evidence that our assumption of the two transitions is correct, since first-order transitions typically display thermal hysteresis. This is a characteristic of re-entrant loops [42]. In addition, our proposed mechanism can explain and it is consistent with the hysteretic behavior displayed by the M vs. H loops presented in Fig. 4. Below, we will describe these loops and discuss their importance.

In Fig. 4 are shown two M vs. H loops that were measured at 280 K. Before the two loops were measured, the alloy sample was subjected to the following thermo-magnetic conditioning. The sample was first cooled from room temperature down to 270 K under zero magnetic field. The temperature was then raised to 280 K, the temperature again equilibrated and each loop was measured. This procedure was used to ensure that the sample was in a demagnetized state before measuring each loop. For the loop shown in Fig. 4a, the field was cycled between zero and plus saturation (4000 kA/m, 5 T); we refer to this loop as the first quadrant loop, whose ascending segment represents the virgin curve. Fig. 4b shows the major loop, where the field was cycled between plus saturation (3980 kA/m, 5 T) and minus saturation (−3980 kA/m, −5 T). Fig. 4a shows that the virgin curve lies considerably below the ascending first quadrant segment of the major loop (Fig. 4b), whereas the descending segments of both loops are essentially superimposed on each other. This difference between the virgin curve and the ascending segment of the major loop gives rise to the large difference in the hysteresis losses in the two loops (compare Fig. 4a and b).

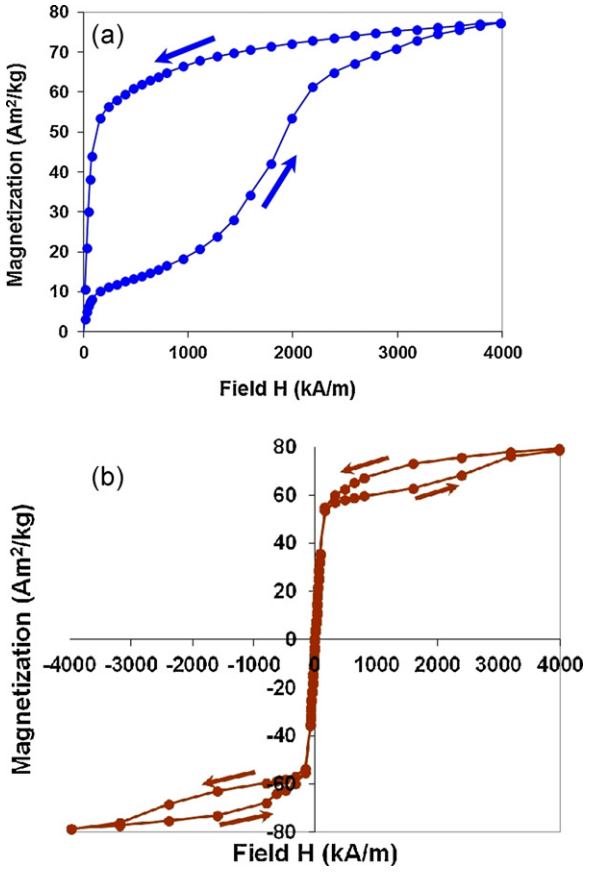

Fig. 4. M vs. H first quadrant loop for the $Ni_{50}Mni_{35}In_{15}$ alloy measured at 280 K, where the applied field was cycled between zero and 3980 kA/m (5 T, saturation) (a); and M vs. H major loop also measured at 280 K by cycling the field between plus saturation (3980 kA/m, 5 T) and minus saturation (−3980 kA/m, −5 T) (b).

We attribute the difference between the virgin curve and the ascending segment of the major loop in to the (irreversible) part of the ferrimagnetic-to-ferromagnetic field-induced transition that is retained in the ferromagnetic state and it does not transform back to the ferrimagnetic state when the field returns to zero both in the cycling of the first quadrant loop and the major loop. It is assumed that the magnetic state of sample at the start of the virgin curve was in the ferrimagnetic state (though a small fraction of the sample might still be in the ferromagnetic state). As the field is increased and it reaches a critical value, the field-induced ferri-to-ferromagnetic transition begins and is mostly completed at the saturation field of 4000 kA/m (5 T). When the field is decreased to zero, through the descending segment of the first quadrant loop, a large fraction of the sample does not transformed to the ferrimagnetic state but it is retained in the ferromagnetic state. This untransformed ferromagnetic fraction is seen in the ascending segment of the major loop in the first quadrant (Fig. 4(b)). Velez et al. demonstrated a similar phenomenon in the M vs. H first quadrant isothermal plots measured at 2 K in a material that is known to undergo an antiferromagnetic-to-ferromagnetic transition at low temperatures [43].

4. Summary and conclusions

Based on our experimental data, a new interpretation for the magnetic behavior of the well-studied $Ni_{50}Mn_{35}In_{15}$ Heusler alloy is presented. A magnetization peak previously identified as a transformation to a ferromagnetic austenite phase is reinterpreted as a spin flipping peak occurring within the martensite phase and representing a Kittel transformation [38]. This Kittel transformation, resulting in a rapid increase in the magnetization value, is the same phenomenon that gives rise to the large inverse MCE peak observed in this alloy, followed by the smaller conventional MCE peak associated with the martensite-to-austenite first-order magnetocrystalline transition at a slightly higher temperature. The influence of this spin flipping peak is also manifested in the unusual behavior observed in the hysteresis loops at 280 K. This behavior encompasses an interesting characteristic of re-entrant loops.

References

[1] F-X. Hu, B-G. Shen, J.R. Sun, Appl. Phys. Lett. 76 (2000) 3460.
[2] P.J. Webster, K.R.A. Ziebeck, S.L. Town, M.S. Peak, Philos. Mag. B 49 (1984) 295.
[3] R. Tickle, R.D. James, J. Magn. Magn. Mater. 195 (1999) 627.
[4] A. Sozinov, A.A. Likhachev, N. Lanska, K. Ullakko, Appl. Phys. Lett. 80 (2002) 1746.
[5] X. Zhou, et al., J. Phys. Condens. Matter 16 (2004) L39.
[6] T. Krenke, M. Acet, E.F. Wassermann, X. Moya, L. Mañosa, A. Planes, Phys. Rev. B 73 (2006) 174413.
[7] Y. Tokura, Y. Tomioka, H. Kuwahara, A. Asamitsu, Y. Moritomo, M. Kasai, J. Appl. Phys. 79 (1996) 5288.

[8] E. Brück, O. Tegus, X.W. Li, K.H.J. Buschow, Physica B 327 (2003) 431.
[9] W.H. Wang, F.X. Hu, J.L. Chen, Y.X. Li, Z. Wang, Z.Y. Gao, Y.F. Zheng, L.C. Zhao, G.H. Wu, W.S. Zan, IEEE Trans. Magn. 37 (2001) 2715.
[10] M. Khan, I. Dubenko, N. Ali, J. Appl. Phys. 97 (2003) 10M304.
[11] S. Stadler, M. Khan, J. Mitchell, N. Ali, A.M. Gomes, I. Dubenko, A.Y. Takeuchi, A.P. Guimarães, Appl. Phys. Lett. 88 (2006) 192511.
[12] F.-X. Hu, B. Shen, J. Sun, G. Wu, Phys. Rev. B 64 (2001) 132412.
[13] L. Pareti, M. Solzi, F. Albertini, A. Paoluzi, Eur. Phys. J. B 32 (2003) 303.
[14] F. Albertini, L. Pareti, A. Paoluzi, L. Morellon, P.A. Algarabel, M.R. Ibarra, L. Righi, Appl. Phys. Lett. 81 (2002) 4032.
[15] I. Babita, M.M. Raja, R. Gopalan, V. Chandrasekaran, S. Ram, J. Alloys Compd. 432 (2007) 23.
[16] X. Zhou, W. Li, H.P. Kunkel, G. Williams, J. Phys.: Condens. Matter 16 (2004) L39.
[17] O. Tegus, E. Brück, L. Zhang, K.H. Dagula, J.F. Buschow, R. de Boer, Physica B 319 (2002) 174.
[18] E. Brück, J. Phys. D: Appl. Phys. 38 (2005) R381.
[19] A.O. Pecharsky, K.A. Gschneidner Jr., V.K. Pecharsky, C.E. Schindler, Alloys Compd. J. 338 (2002) 126.
[20] V.K. Pecharsky, K.A. Gschneidner Jr., J. Magn. Magn. Mater. 200 (1999) 44.
[21] K. Prokeš, O. Tegus, E.J.C. Brück, P.F. Klaasse, R.K.H. de Boer, J. Buschow, J. Alloys Compd. 335 (2002) 62.
[22] T.T.M. Palstra, J.A. Mydosh, G.J. Nieuwenhuys, A.M. van der Kraan, K.H.J. Buschow, J. Magn. Magn. Mater. 36 (1983) 290.
[23] H. Feng-xia, S. Bao-gen, S. Ji-rong, Z. Xi-xiang, Chin. Phys. 9 (2000) 550.
[24] F.X. Hu, B.G. Shen, J.R. Sun, A.B. Pakhomov, C.Y. Wong, X.X. Zhang, S.Y. Zhang, G.J. Wang, Z.H. Cheng, IEEE Trans. Magn. 37 (2002) 1276.
[25] T. Krenke, E. Duman, M. Acet, E.F. Wassermann, X. Moya, L. Mañosa, A. Planes, E. Suard, B. Oulaaddiaf, Phys. Rev. B 75 (2007) 104414.
[26] V.K. Sharma, M.K. Chattopadhyay, R. Kumar, T. Ganguli, P. Tiwari, S.B. Roy, J. Phys.: Condens. Matter 19 (2007) 496207.
[27] H. Wada, Y. Tanabe, Appl. Phys. Lett. 79 (2001) 3302.
[28] V.K. Sharma, J.D. Moore, M.K. Chattopadhyay, K. Morrison, L.F. Cohen, S.B. Roy, J. Phys. D: Appl. Phys. 40 (2007) 1869.
[29] P.A. Bhobe, K.R. Priolkar, A.K. Nigam, Appl. Phys. Lett. 91 (2007) 242503.
[30] S.Y. Yu, Z.H. Liu, G.D. Liu, J.L. Chen, Z.X. Cao, G.H. Wu, B. Zhang, X.X. Zhang, Appl. Phys. Lett. 89 (2006) 162503.
[31] V.K. Sharma, J.D. Moore, M.K. Chattopadhyay, K. Morrison, L.F. Cohen, S.B. Roy, J. Phys. Condens. Matter 22 (2010) 016008.
[32] A.K. Pathak, M. Khan, I. Dubenko, S. Stadler, N. Ali, Appl. Phys. Lett. 90 (2007) 262504.
[33] S.B. Roy, G.K. Perkins, M.K. Chattopadhyay, A.K. Nigam, K.J.S. Sokhey, P. Chaddah, A.D. Caplin, L.F. Cohen, Phys. Rev. Lett. 92 (2004) 147203.
[34] B. Li, W.J. Ren, Q. Zhang, X.K. Lv, X.G. Liu, H. Meng, J. Li, D. Li, Z.D. Zhang, Appl. Phys. Lett. 95 (2009) 172506.
[35] P.A. Bhobe, K.R. Priolkar, P.R. Sarode, J. Phys. D: Appl. Phys. 41 (2008) 045004.
[36] P.A.K. Bhobe, R. Priolkar, A.K. Nigam1, J. Phys. D: Appl. Phys. 41 (2008) 235006.
[37] S. Aksoy, M. Acet, P.P. Deen, M. Mañosa, A. Planesd, Phys. Rev. B 79 (2009) 212401.
[38] C. Kittel, Phys. Rev. 126 (1960) 335.
[39] T. Tohei, H. Wada, T. Kanomata, Appl. Phys. J. 94 (2003) 1800.
[40] O. Tegus, et al., IEEE Trans. Magn. 37 (2001) 2169.
[41] C. Kuhrt, T. Schitty, K. Barner, Phys. Status Solidi A 91 (1985) 105.
[42] V. Basso, C.P. Sasso, G. Bertotti, M. LoBue, Physica B: Condens. Matter 443 (2–3) (2008) 312.
[43] S. Velez, J.M. Hernandez, A. Fernandez, F. Macia, C. Magen, P.A. Algarabel, J. Tejada, E.M. Chudnovsky, Phys. Rev. B 81 (2010) 064437.